Flavor dependence of the chiral phase transition in strong-coupling QCD

Neven Bilić
Fakultät für Physik, Universität Bielefeld, Postfach 8640, D-4800 Bielefeld 1, Germany
and Rudjer Bošković Institute, P.O. Box 1016, 41001 Zagreb, Croatia

Frithjof Karsch
Fakultät für Physik, Universität Bielefeld, Postfach 8640, D-4800 Bielefeld 1, Germany
and HLRZ, Forschungszentrum Jülich, Postfach 1913, D-5170 Jülich, Germany

Krzysztof Redlich
Fakultät für Physik, Universität Bielefeld, Postfach 8640, D-4800 Bielefeld 1, Germany
and Department of Theoretical Physics, University of Wroclaw, Poland
(Received 29 October 1991)

We have studied the chiral phase transition in SU(3) lattice gauge theory with f species of staggered fermions at nonzero chemical potential and temperature. The results at infinite coupling are improved by adding systematic $1/g^2$ corrections. At zero chemical potential we find a flavor dependence of the chiral transition which is in qualitative agreement with Monte Carlo data. At zero temperature, however, the chiral transition turns out to be flavor independent. The thermodynamics of the chiral-symmetric and broken phases is discussed in detail.

PACS number(s): 12.38.Gc, 05.70.Jk, 11.30.Rd

I. INTRODUCTION

Monte Carlo simulations of strong-coupling QCD [1–3] have shown that the mean-field analysis of large-d or large-N approximations of the QCD partition function [4–6] leads to a rather good quantitative description of the phase diagram in the finite-temperature and finite-chemical-potential plane. This includes the order of the phase transition as well as the location of the critical couplings. It yields a second-order phase transition at finite temperature (T) and vanishing chemical potential (μ) and predicts a first-order transition for any nonzero value of μ, in agreement with Monte Carlo data. Of course, the mean-field analysis does not lead to the correct critical exponents of strong-coupling QCD [7].

A rather striking feature of QCD Monte Carlo simulations is the strong flavor dependence of the order of the chiral phase transition as well as its temperature dependence [8]. The former seems to follow closely the pattern expected from the analysis of the phase structure of general effective three-dimensional (3-d) chiral Lagrangians [9], which also has been confirmed in numerical studies of these effective models [10]. The flavor dependence of the transition temperature has been studied in the mean-field approach for the case of U(N) gauge groups for $\mu=0$, $\beta=0$ [11]. In the present paper we will extend this analysis to the case of SU(3) for $\mu=0$ as well as $\mu>0$ and we will include first order corrections in $1/g^2$, which previously have been calculated only for the case of one species of staggered fermions [6, 12].

The main result of this analysis is a flavor dependence of the finite temperature transition temperature at $\mu=0$, which is in qualitative agreement with Monte Carlo data, and a flavor-independent transition as a function of μ at zero temperature. This led us to reexamine the nature of the chiral transition at zero temperature, which has been puzzling for quite some time [2, 4, 13–17]. We conclude that at zero temperature the chiral transition coincides with the threshold effect, describing the transition from the ordinary QCD vacuum without baryons to a state of extended nuclear matter with finite baryon-number density. The critical value of the chemical potential is a direct measure for the binding energy of nuclear matter.

The paper is organized as follows. In Sec. II we describe the application of the mean-field method to strong coupling QCD with f species of staggered fermions ($f=1,2,\ldots$) at nonzero μ and nonzero T and discuss the $O(1/g^2)$ corrections. In Sec. III we study the flavor dependence of the critical temperature at $\mu=0$. In Sec. IV we discuss the chiral phase transition at nonzero μ and the thermodynamics of the two phases. Finally, in Sec. V the concluding remarks are presented. Some further technical details concerning the analytic formulas used in our calculations are given in Appendixes A and B.

II. EFFECTIVE PARTITION FUNCTION AND MEAN-FIELD METHOD

Our starting point is the effective partition function derived at infinite coupling and in the large-d limit [12, 18–20] generalized to an arbitrary number of Kogut-Susskind flavors f:

$$Z_{\text{eff}}=\int \prod_{t \text{ links}} [dU] \prod_{x,a} [d\bar{\chi}_a(x) d\chi_a(x)] \exp\left[-\sum_{x,y} \bar{\chi}_a(x) \left[m\delta_{x,y} + \frac{\gamma}{2} a_x U_{xy} \delta_{x,y-\hat{\imath}} - \frac{\gamma}{2} b_x U_{xy}^{\dagger} \delta_{x,y+\hat{\imath}} \right] \chi_a(y) - \sum_{\langle x,y \rangle} A_f(x,y) \right] , \tag{2.1}$$

where $\langle x,y \rangle$ denotes spatially neighboring sites at equal time. $A_f(x,y)$ is a finite-order polynomial in the variables $\bar{\chi}_a(x)\chi_b(x)$ and $\bar{\chi}_c(y)\chi_d(y)$:

$$A_f(x,y)=\frac{1}{4N}\bar{\chi}_a(x)\chi_b(x)\bar{\chi}_b(y)\chi_a(y) + \frac{1}{32N(N^2-1)} \left[\frac{1}{N} [\bar{\chi}_a(x)\chi_b(x)\bar{\chi}_b(y)\chi_a(y)]^2 + \bar{\chi}_a(x)\chi_b(x)\bar{\chi}_b(y)\chi_c(y)\bar{\chi}_c(x)\chi_d(x)\bar{\chi}_d(y)\chi_a(y) \right] + \cdots . \tag{2.2}$$

Summation over repeating flavor indices a, b, c, and d is understood. The first and the second term in (2.2) are the leading and the next-to-leading orders in a systematic large d expansion, respectively. All other terms are successively $1/d$ suppressed [21]. We work on an asymmetric lattice with N_t points in the time direction and N_s points in the d space directions with an anisotropy γ. In the naive continuum limit γ can be interpreted as a ratio of the space and timelike lattice spacings:

$$\gamma=\frac{a_s}{a_t} . \tag{2.3}$$

The finite-temperature behavior will be studied in the infinite-volume limit ($N_s \to \infty$) as a function of γ and N_t. The parameters a_x and b_x at each space-time point x are usually set equal to the constants a and b related to the chemical potential. The most convenient prescription is

$$a=e^{\mu}, \quad b=e^{-\mu} . \tag{2.4}$$

We now apply the mean-field ansatz by replacing each of the $2d$ spatial neighbors of the fermionic pair $\bar{\chi}_a\chi_b$ at a site x by a constant *mean field* λ:

$$\bar{\chi}_b(y)\chi_a(y) \to \frac{4N}{2d}\lambda\delta_{ba} . \tag{2.5}$$

Keeping only the first term in Eq. (2.2) the interaction is then linearized and the integration over $\bar{\chi}_a(x)$ and $\chi_a(x)$ can be performed. The partition function factorizes into a product of "one-dimensional" partition functions at each space point $\mathbf{x}$:

$$Z_f=\int dU [\det D(U)]^f , \tag{2.6}$$

with $D(U)$ being an $N_t N \times N_t N$ matrix:

$$D(\mathrm{U})=\begin{bmatrix} 2(\lambda_1+m)\mathbb{1} & \gamma a_1 \mathbb{1} & 0 & \cdots & \gamma b_{N_t} U^{\dagger} \\ -\gamma b_1 \mathbb{1} & 2(\lambda_2+m)\mathbb{1} & \gamma a_2 \mathbb{1} & & 0 \\ 0 & -\gamma b_2 \mathbb{1} & 2(\lambda_3+m)\mathbb{1} & & 0 \\ \vdots & & & \ddots & \\ -\gamma a_{N_T} U & 0 & 0 & & 2(\lambda_{N_t}+m)\mathbb{1} \end{bmatrix} . \tag{2.7}$$

Here the $\mathbf{x}$ dependence has been omitted and the mean-field λ has been allowed to vary in time points. The integration over dU is performed by exploiting the appropriate SU(N) group integral. The results for $f=1$, 2, and 3 we give in Appendix A. In the final expressions we put

$$\lambda_1=\lambda_2=\cdots=\lambda_{N_t}=\lambda , \tag{2.8}$$

$$a_1=a_2\cdots=a_{N_t}=e^{\mu}, \quad b_1=b_2\cdots=b_{N_t}=e^{-\mu} .$$

The mean-field consistency requires

$$\frac{1}{Z_f}\frac{\partial Z_f}{\partial\lambda}=N_t\frac{2fN}{d}\lambda . \tag{2.9}$$

Solving Eq. (2.9) is equivalent to minimizing the mean-field free energy defined as

$$F=\frac{N_t f N}{d}\lambda^2-\ln Z_f . \tag{2.10}$$

We improve infinite-coupling calculations by replacing the mean-field free energy (2.10) by

$$F \to F-\sum_{i=1}^{5}\delta F_i , \tag{2.11}$$

with δF_i being corrections of order $1/g^2$ or $1/d$ [12]. These corrections are obtained from the expansion of the gauge sector combined with the fermion sector in the full partition function. For $f=1$ one can express δF_i in terms of derivatives of the partition function Z_1 given in

(2.6) with respect to a_i, b_i, and λ_i [6, 12]. In Appendix B we show that for arbitrary number of flavors f the same procedure leads to similar expressions with additional color- and flavor-dependent factors. From (B16)–(B19) we have

$$\delta F_1=\frac{2N_t d}{fN\gamma^2}\beta_t\left[\frac{\partial Z_f}{\partial a}\Big/Z_f\right]\left[\frac{\partial Z_f}{\partial b}\Big/Z_f\right], \tag{2.12}$$

$$\delta F_2=\frac{N_t d(d-1)}{f^3N^3}\beta_s\left[\frac{1}{2}\frac{\partial Z_f}{\partial\lambda}\Big/Z_f\right]^4, \tag{2.13}$$

$$\delta F_3=\frac{4N_t d(N^2-1)}{N^2(fN-1)^2\gamma^2}\beta_t \times\left[\frac{1}{2}\frac{\partial^2 Z_f}{\partial a\partial\lambda}\Big/Z_f\right]\left[\frac{1}{2}\frac{\partial^2 Z_f}{\partial b\partial\lambda}\Big/Z_f\right], \tag{2.14}$$

$$\delta F_4=\frac{N_t d(N-f)}{2N^2 f(fN-1)^2}\left[\frac{1}{4}\frac{\partial^2 Z_f}{\partial\lambda^2}\Big/Z_f\right]^2, \tag{2.15}$$

$$\delta F_5=\frac{N_t d}{8N^2}\left[\frac{1}{2}\frac{\partial^2\ln Z_f}{\partial\lambda^2}\right]^2, \tag{2.16}$$

with

$$\beta_s=\frac{1}{g_s^2N\gamma}\,,\quad \beta_t=\frac{\gamma}{g_t^2N}\,, \tag{2.17}$$

where g_s and g_t are the coupling constants associated to the spacelike and timelike plaquettes in the gauge sector of the lattice action. δF_4 and δF_5 are the corrections of the same order in $1/d$. δF_4 is a contribution due to the next-order term in (2.2) and δF_5 is a contribution obtained by integration of quadratic fluctuations around the mean-field solution [21]. Analytic expressions for the derivatives of Z_f are given in Appendix A.

We note that δF_1 and δF_3 behave like $O(\lambda^2)$ for small λ whereas all other terms are of order λ^4. Therefore only δF_1 and δF_3 influence the location of the second-order phase transition which we discuss in the next section.

III. PHASE TRANSITION AT ZERO CHEMICAL POTENTIAL

In this section we discuss the f dependence of the critical temperature at the point of second-order phase transition predicted at strong coupling. At zero temperature, chiral symmetry is broken for any value of the anisotropy parameter γ. For fixed N_t there exists a chiral-symmetry-restoring phase transition at some value γ_c, with $\gamma_c\to\infty$ if $N_t\to\infty$. We thus can vary the temperature of the system by varying the coupling γ on a lattice with fixed N_t. However, unlike the weak-coupling regime, where the anisotropy parameter can directly be related to the spatial and temporal lattice spacings [22] and thus allows one to establish a connection between γ and the temperature $T=1/N_t a_t$, such a direct relation does not exist in the strong-coupling limit.

The location of the critical point is determined by the properties of the mean-field free energy. For $\mu=0$ our mean-field free energy is an even function of λ. Even after including corrections of order $1/d$ and $1/g^2$, Eq. (2.2), the transition stays second order. As our action has a global $U(f)\times U(f)$ chiral symmetry, the general analysis of [9] would suggest a first-order transition to occur for $f\geq 3$. At present we cannot exclude that the reason for the difference in our findings is an artifact of the mean-field analysis. However, there is also the possibility that in our case the effective 3-d Lagrangian, which is expected to control the order of the chiral phase transition, is not yet of the general form considered in Ref. [9]. It may be restricted to an $O(2f)$-invariant subspace, which can give rise to second-order phase transitions. A detailed analysis of critical exponents, which is beyond the scope of our present mean-field analysis, would thus be interesting in order to clarify this point.

The chiral symmetry is restored if

$$\left.\frac{\partial^2 F}{\partial\lambda^2}\right|_{\lambda=0}\geq 0\,, \tag{3.1}$$

since in this case $\lambda=0$ is a true minimum. The second order phase transition takes place at the point when (3.1) becomes an equality. From Eq. (2.10) together with (2.11)–(2.16) and using Eqs. (A8)–(A13) we find the following expression for F in the neighborhood of $\lambda=0$:

$$F=\frac{fN_tN}{d}\left[1-\frac{\gamma_0^2}{\gamma^2}+\beta_t\left[2d-f\frac{N^2-1}{N}\frac{\gamma_0^2}{\gamma^2}\right]\frac{\gamma_0^2}{\gamma^4}\right]\lambda^2 +O(\lambda^4)\,, \tag{3.2}$$

with

$$\gamma_0^2=\frac{N_t}{f}\frac{1}{Z_f}\frac{\partial Z_f}{\partial h}\bigg|_{\lambda=0} \tag{3.3}$$

being the critical anisotropy at infinite coupling. The derivative in (3.3) is taken with respect to the parameter h defined in Appendix A. At the transition point the expression in square brackets in Eq. (3.2) should vanish, yielding the critical anisotropy as a function of β_t:

$$\gamma_c^2=\gamma_0^2-\beta_t\left[2d-f\frac{N^2-1}{N}\right]. \tag{3.4}$$

We note that the correction to the critical anisotropy does not depend on N_t although γ_0^2 itself is proportional to N_t. For $f=1$ the critical anisotropy at infinite coupling γ_0 takes on the values

$$\gamma_0^2=\frac{d(N+2)}{6}N_t \tag{3.5}$$

for U(N) [11], and

$$\gamma_0^2=\frac{d(N+1)(N+2)}{6(N+3)}N_t \tag{3.6}$$

for SU(N) [12] gauge groups. We show γ_0^2 as a function of f for both U(3) and SU(3) in Fig. 1. For noninteger values of f we have used a numerical integration of the group integral (2.6). The decrease of the critical lattice anisotropy γ_0 with f roughly fits $f^{-1/2}$ for $f<2$, as suggested by the chiral-Lagrangian models [23, 24]. For a

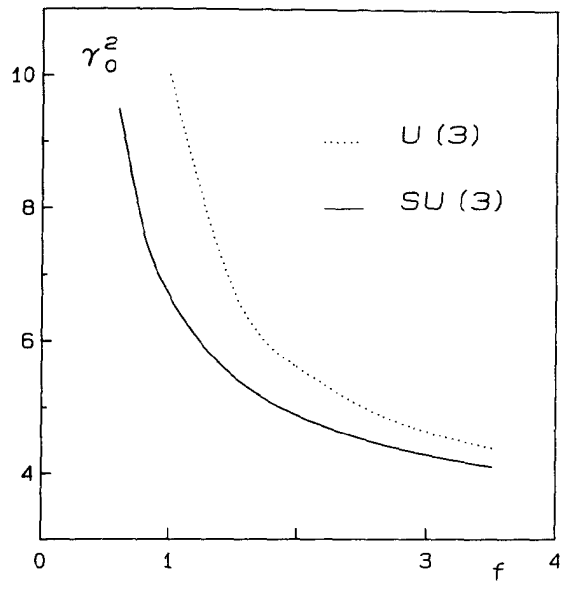

FIG. 1. Critical lattice anisotropy as a function of flavor number f.

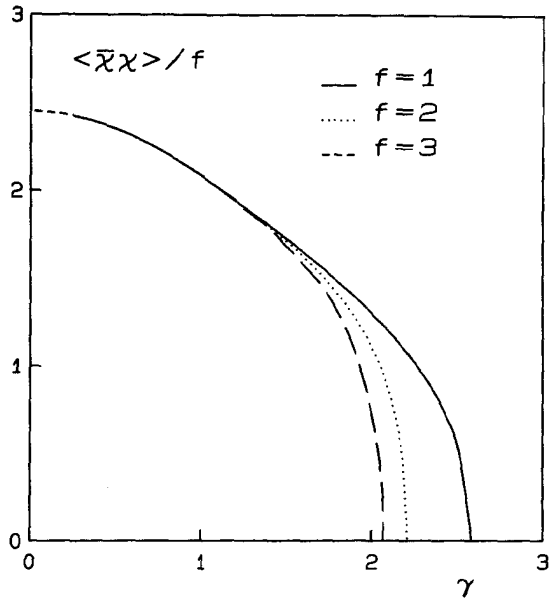

FIG. 2. Chiral condensate as a function of lattice anisotropy parameter for various flavor numbers f.

large number of flavors the decrease is, however, much weaker. We note that the finite $1/g^2$ correction in (3.4) has an opposite trend; i.e., the correction term decreases with f and becomes even negative for $f > \frac{9}{4}$, which in turn produces an increase of γ_c. This may indicate a poor convergence of the $1/g^2$ expansion for large f, which could be a first hint for the appearance of a first-order transition for $f \geq 3$ [9] or even indicate the existence of a bulk transition in QCD with a large number of flavors, which could occur before the chiral transition takes place [25]. In total, however, we find that the correction is small and only slightly modifies the leading term.

Another effect of the strong coupling corrections is that for $f=1$ and 2 the "critical temperature" decreases with increasing $1/g^2$. This decrease, however, is not sufficient to fit the Monte Carlo (intermediate coupling) data for $N_t=4$.

IV. PHASE STRUCTURE OF THE CHIRAL TRANSITION

In this section we find a numerical solution to the mean-field equation

$$\frac{\partial F}{\partial \lambda}=0 , \tag{4.1}$$

with F defined in Eqs. (2.10) and (2.11) in the chiral limit ($m \to 0$) for arbitrary values of μ. The solution gives the value of the mean field λ which is related to the chiral condensate through Eq. (2.5):

$$\langle \bar{\chi}_a \chi_a \rangle = \frac{2fN}{d}\lambda . \tag{4.2}$$

In Fig. 2 we plot our solution for $\mu=0$ and $N_t=4$. The chiral condensate as a function of γ shows a second-order phase transition. The transition stays second order even when $1/g^2$ corrections are included. For $N_t < \infty$ a chiral-symmetry-restoring transition takes place at the value of γ given by Eq. (3.4).

We next consider nonzero chemical potential. In this case the chiral phase transition, predicted by the mean-field method, becomes first order [6]. The critical value of the chemical potential as a function of γ we find by solving Eq. (4.1) numerically, with F given by (2.10). The phase diagrams for three values of f are shown in Fig. 3. We observe a stronger f dependence when the transition point approaches the critical point at $\mu=0$. The $1/g^2$ corrections do not change the qualitative structure of the phase diagrams.

Let us now discuss the limit $N_t \to \infty$ corresponding to the zero-temperature limit. Using (A15)–(A25), we find a nontrivial solution to the mean-field equation (4.1) which

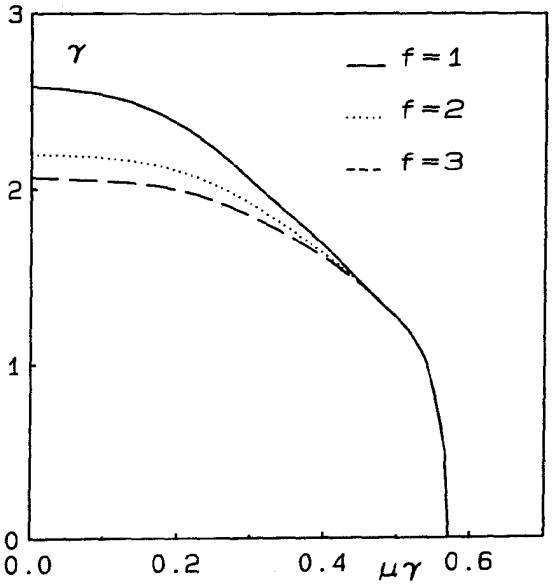

FIG. 3. Phase diagram of the chiral transition for various flavor numbers f.

in the strong-coupling and large-d limit can be approximated by

$$\bar{\lambda}=\lambda_0\left[1-\frac{\beta_s}{2}-\frac{1}{4d}+\frac{\beta_s}{2d}-\frac{\beta_t}{d}\left[1+\frac{3f}{2d}\frac{N^2-1}{N}\right]\right] \quad (4.3)$$

for all $\mu \leq \operatorname{arcsinh}(\bar{\lambda}/\gamma)$, with

$$\lambda_0=\frac{1}{\sqrt{2}}(\sqrt{\gamma^4+d^2}-\gamma^2)^{1/2}, \quad (4.4)$$

being the solution at infinite coupling [5]. As soon as μ becomes greater than $\operatorname{arcsinh}(\bar{\lambda}/\gamma)$ only the trivial solution, $\lambda=0$, survives.

The chiral transition takes place at the chemical potential $\bar{\mu}$ obtained from the requirement

$$F(0)=F(\bar{\lambda}), \quad (4.5)$$

which yields

$$\bar{\mu}=\operatorname{arcsinh}(\bar{\lambda}/\gamma)-\frac{\bar{\lambda}^2}{d}+\frac{\beta_s}{4}+\frac{1}{8d}-\frac{\beta_s}{4d}+\frac{\beta_t}{2d}\left[1+\frac{f}{d}\frac{N^2-1}{N}\right]. \quad (4.6)$$

In Eqs. (4.3) and (4.6) we keep the dominant $1/d$ and $1/g^2$ corrections only, and the lowest order f-dependent term which is $1/d$ suppressed but color enhanced. We note that for $\gamma=1$ the systematic $1/d$ and $1/g^2$ expansion for the critical chemical potential gives

$$\bar{\mu}|_{\gamma=1}=\frac{1}{N}m_N-\Delta, \quad (4.7)$$

with

$$m_N=\ln(2d)^{N/2}-\frac{N}{4d}-\frac{1}{2g^2}, \quad (4.8)$$

being the strong-coupling nucleon mass calculated to the same order in $1/d$ and $1/g^2$ [21, 26], and

$$\Delta=\frac{\bar{\lambda}^2}{d}-\frac{1}{4Ng^2}-\frac{1}{8d}. \quad (4.9)$$

The reason for writing $\bar{\mu}$ in this way will become obvious from a consideration of the thermodynamics.

In order to understand better the thermodynamics of our model let us now discuss the pressure and the energy density. The pressure is defined as

$$P=-\frac{F_{\min}}{N_t}-P_{\text{vac}}, \quad (4.10)$$

with $F_{\min}$ being the minimum of the single-site mean-field free energy (2.10) for given γ and μ. The subtracted vacuum pressure is calculated at $T=\mu=0$ using the $N_t\to\infty$ limit of Z_f derived in Appendix A:

$$P_{\text{vac}}=fN\bar{\mu}, \quad (4.11)$$

with $\bar{\mu}$ being the transition chemical potential at zero temperature (4.6).

We plot the pressure as a function of μ for $f=1$ in Fig. 4 and for $f=1$, 2, and 3 in Fig. 5. In Fig. 4 we give the

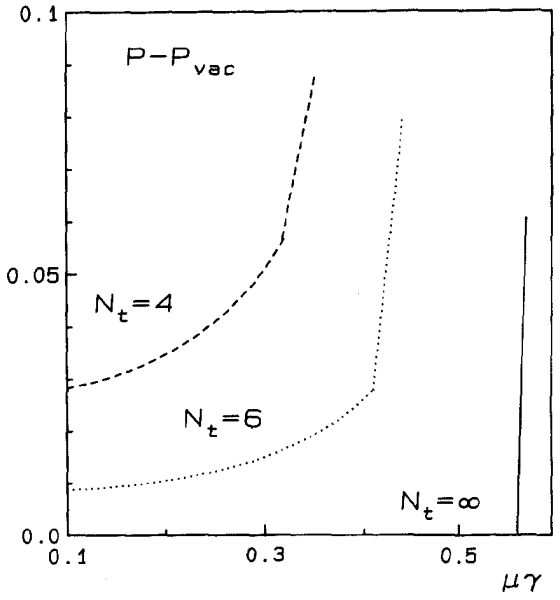

FIG. 4. Pressure as a function of chemical potential for fixed $\gamma=2$ and for various temporal sizes of the lattice.

$N_t\to\infty$ result corresponding to the zero temperature and the $N_t=4$ and 6 results at finite temperature for $\gamma=2$. The behavior of the pressure is typical for the first-order phase transition. Figure 5 shows that the phase transition at finite μ becomes weaker first order with increasing f. This can easily be understood from the phase diagram shown in Fig. 3. By increasing f at fixed γ we come closer to the second-order phase transition at $\mu_c=0$.

Next we consider the energy per baryon in the zero-temperature limit near the transition point $\bar{\mu}$ given by Eq. (4.6). The baryon-number density we define as

$$n_B=-\frac{1}{N_tN}\frac{\partial F_{\min}}{\partial\mu}, \quad (4.12)$$

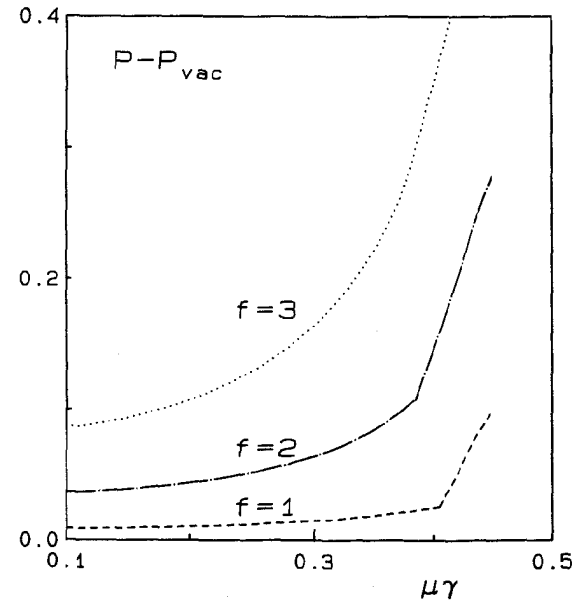

FIG. 5. Pressure as a function of chemical potential for fixed $\gamma=1.5$ and for various flavor numbers.

and the energy density as

$$\mathcal{E}=\left.\frac{\partial F_{\min}}{\partial N_t}\right|_{\mu N_t} . \tag{4.13}$$

The energy density is usually defined as a derivative of the free energy with respect to γ which in the weak coupling regime is related to the temperature. However, as we have already mentioned, such a direct relation does not exist in the strong-coupling limit. In fact, the relations (3.5, 3.6) suggest that in the strong coupling limit $\gamma^2 \sim T$ is a more natural relation. We therefore use the definition (4.13) which is independent of the interpretation of γ. In the definitions (4.12, 4.13) we have omitted inessential dimensional factors. In the limit $N_t \to \infty$ the energy per baryon near the threshold $\bar{\mu}$ is then given by

$$\frac{\mathcal{E}-\mathcal{E}_{\text{vac}}}{n_B}=\begin{cases} N\,\text{arcsinh}\left[\dfrac{\bar{\lambda}}{\gamma}\right] & \text{if } \mu<\bar{\mu} , \\ N\bar{\mu} & \text{if } \mu>\bar{\mu} . \end{cases} \tag{4.14}$$

Thus, in the chiral-symmetry-broken phase the energy per baryon near the threshold equals the value of the lightest baryon mass in the large-d limit [21, 26]. On the other hand, in the symmetric phase it approaches the transition value of the chemical potential multiplied by N.

Let us compare our results with an ideal gas of massive baryons. The energy per baryon of such a system is given by [27]

$$\frac{\mathcal{E}-\mathcal{E}_{\text{vac}}}{n_B}=\frac{\int_0^\infty dp\, p^2\sqrt{p^2+m^2}\left[\exp\left[\dfrac{\sqrt{p^2+m^2}-\mu}{T}\right]+1\right]^{-1}}{\int_0^\infty dp\, p^2\left[\exp\left[\dfrac{\sqrt{p^2+m^2}-\mu}{T}\right]+1\right]^{-1}} , \tag{4.15}$$

which in the limit $T \to 0$ near the threshold m yields

$$\frac{\mathcal{E}-\mathcal{E}_{\text{vac}}}{n_B}=\begin{cases} m & \text{if } \mu<m \\ \mu-\dfrac{2}{5}(\mu-m)+O((\mu-m)^2) & \text{if } \mu>m . \end{cases} \tag{4.16}$$

This result obviously reflects the fact that the threshold value of the chemical potential of an ideal gas of massive baryons at zero temperature equals the baryon mass. In strong-coupling QCD, however, there is a difference between two limiting values of the energy per baryon due to interaction. This difference, which in the large-d limit precisely equals the difference between the strong-coupling nucleon mass and the chemical-potential threshold, may be interpreted as a binding energy of nuclear matter. It should, however, be noted that at $\mu=\bar{\mu}$ the number density jumps directly from zero to the maximal value $n_B=1$ corresponding to three quarks per site on the lattice. Since baryons are also localized to single sites in the strong-coupling limit we cannot distinguish a high-density nuclear matter phase from a quark-gluon-plasma phase. One eventually expects that in the continuum limit two "transitions" show up as a function of μ at $T=0$. The first one is a threshold effect corresponding to the transition from the QCD vacuum to a state of extended nuclear matter and should be first order. The second one, occurring at a larger value of μ, corresponds to the chiral-phase transition from hadronic matter to a quark-gluon plasma.

V. CONCLUSIONS

In our analysis we have found that the structure of finite μ and finite T chiral transition at strong coupling may quantitatively and qualitatively change when the number of flavors change. At infinite coupling the effect is more pronounced for small number of flavors (Fig. 1). We find a flavor dependence of the finite-temperature transition at $\mu=0$, which is in qualitative agreement with Monte Carlo data, and a flavor-independent transition as a function of μ at zero temperature. As is clearly seen from Figs. 2 and 3, the flavor effects on the chiral condensate are more pronounced at temperatures and chemical potentials closer to the critical point.

By analyzing the thermodynamical quantities such as pressure and energy density we conclude that at zero temperature the chiral transition is a threshold effect, describing the transition from the ordinary QCD vacuum without baryons to a state of extended nuclear matter with finite baryon number density. At least in strong-coupling QCD there is no low-density, chiral-symmetry-broken gas phase of nucleons. The threshold value of the chemical potential is a direct measure for the binding energy of nuclear matter, which is large in the strong-coupling limit.

We have also found that the $1/d$ dominant part of the $1/g^2$ corrections to the critical temperature does not depend on f. The effect of this term is to lower the critical temperature approaching thus correctly the weak-coupling regime. However, the part of the corrections which is subdominant in $1/d$ and has the sign opposite to the dominant term, is proportional to f. The overall effect is that for f between two and three the corrections change sign suggesting more complicated structure of the chiral transition for systems with large number of flavors.

ACKNOWLEDGMENTS

We would like to thank H. Satz, B. Petersson, and K. Demeterfi for useful discussions and help.

APPENDIX A: PARTITION FUNCTION AND ITS DERIVATIVES

In this section we calculate the partition function and its derivatives for $f=1$, 2, and 3 for the SU(3) group and arbitrary $n \equiv N_t$ and for the SU(N) group in the limit $n \to \infty$ using general formulas derived in Ref. [12]. We use the notation

$$\hat{a}=\prod_{i=1}^{n} a_i, \quad \hat{b}=\prod_{i=1}^{n} b_i, \qquad \text{(A1)}$$

$$\alpha_i=a_i b_i, \quad I_i=2(\lambda_i+m)/\gamma \ .$$

Evaluation of the group integral (2.6) yields in general

$$Z_f=\sum_{i+j+k=fN} C_{ijk}\hat{a}^i\hat{b}^j h^k \qquad \text{(A2)}$$

and, in particular for $N=3$ and $f=1$, 2, and 3,

$$Z_1=h^3-2\hat{a}\hat{b}h+\hat{a}^3+\hat{b}^3 \ , \qquad \text{(A3)}$$

$$Z_2=h^6-2\hat{a}\hat{b}h^4+4(\hat{a}^3+\hat{b}^3)h^3+3\hat{a}^2\hat{b}^2h^2-6(\hat{a}^3+\hat{b}^3)\hat{a}\hat{b}h+\hat{a}^6+\hat{b}^6+6\hat{a}^3\hat{b}^3 \ , \qquad \text{(A4)}$$

$$\begin{aligned} Z_3=&h^9+10\hat{b}^3h^6+10\hat{a}^3h^6+9\hat{a}^2\hat{b}^2h^5-15\hat{a}\hat{b}^4h^4-15\hat{a}^4\hat{b}h^4 \\ &+10\hat{b}^6h^3+36\hat{a}^3\hat{b}^3h^3+10\hat{a}^6h^3+18\hat{a}^2\hat{b}^5h^2+18\hat{a}^5\hat{b}^2h^2 \\ &-12\hat{a}\hat{b}^7h-54\hat{a}^4\hat{b}^4h-12\hat{a}^7\hat{b}h+\hat{b}^9+18\hat{a}^3\hat{b}^6+18\hat{a}^6\hat{b}^3+\hat{a}^9 \ , \end{aligned} \qquad \text{(A5)}$$

where h as a function of $I_1,\ldots,I_n$ and $\alpha_1,\ldots,\alpha_n$ is defined by

$$h=B_n(I_1,\ldots,I_n;\ \alpha_1,\ldots,\alpha_{n-1})+\alpha_n B_{n-2}(I_2,\ldots,I_{n-1};\ \alpha_2,\ldots,\alpha_{n-2}) \ , \qquad \text{(A6)}$$

with B_n being the $n\times n$ determinant:

$$B_n(I_1,\ldots,I_n;\ \alpha_1,\ldots,\alpha_{n-1})=\begin{vmatrix} I_1 & a_1 & 0 & \cdots & & 0 \\ -b_1 & I_2 & a_2 & & & 0 \\ 0 & -b_2 & I_3 & & & 0 \\ \vdots & & & \ddots & & \\ & & & & I_{n-1} & a_{n-1} \\ 0 & 0 & 0 & & -b_{n-1} & I_n \end{vmatrix} . \qquad \text{(A7)}$$

The derivatives of Z_f can be easily calculated using (A3)–(A5) with (A6) and (A7). In the final expressions the parameters a_i, b_i, and λ_i are set equal to the values given in Eq. (2.8). In this case we have

$$h=2\cosh(n\lambda') \ , \qquad \text{(A8)}$$

$$\frac{\partial h}{\partial \alpha_i}=\frac{\cosh[(n-1)\lambda']}{\cosh\lambda'} \ , \qquad \text{(A9)}$$

$$\frac{\partial h}{\partial \lambda_i}=\frac{2}{\gamma}\frac{\sinh(n\lambda')}{\cosh\lambda'} \ , \qquad \text{(A10)}$$

with

$$\lambda'=\operatorname{arcsinh}[(\lambda+m)/\gamma] \ . \qquad \text{(A11)}$$

In the special case when $\mu=0$ and $\lambda=0$ from Eq. (A2) we find the useful relations

$$\frac{\partial Z_f}{\partial \hat{a}}+\frac{\partial Z_f}{\partial \hat{b}}+2\frac{\partial Z_f}{\partial h}=fNZ_f \ , \qquad \text{(A12)}$$

$$\frac{\partial^2 Z_f}{\partial \hat{a}\partial h}+\frac{\partial^2 Z_f}{\partial \hat{b}\partial h}+2\frac{\partial^2 Z_f}{\partial h^2}=(fN-1)\frac{\partial Z_f}{\partial h} \ . \qquad \text{(A13)}$$

The $n\to\infty$ limit of Z_f and its derivatives can be derived for arbitrary N and f using the asymptotic form

$$Z_f=(\hat{a}^{fN}+\hat{b}^{fN}+h^{fN})[1+\epsilon(n)] \ , \qquad \text{(A14)}$$

where $\epsilon(n)$ denotes the terms vanishing exponentially with n. Applying the $n\to\infty$ limit to Eqs. (A8)–(A11) we find the limiting values of $\ln Z_f$ and its derivatives in the two regimes depending on the magnitude of λ' with respect to μ.

(1) $\lambda'>\mu$:

$$\left[\frac{1}{n}\ln Z_f\right]_{n\to\infty}=fN\lambda' \ , \qquad \text{(A15)}$$

$$\left[\frac{1}{Z_f}\frac{\partial Z_f}{\partial a}\right]_{n\to\infty}=fN\frac{e^{-\lambda'}}{2\cosh\lambda'}e^{-\mu} \ , \qquad \text{(A16)}$$

$$\left[\frac{1}{Z_f}\frac{\partial Z_f}{\partial b}\right]_{n\to\infty}=fN\frac{e^{-\lambda'}}{2\cosh\lambda'}e^{\mu} \ , \qquad \text{(A17)}$$

$$\left[\frac{1}{Z_f}\frac{\partial Z_f}{\partial \lambda}\right]_{n\to\infty}=fN\frac{1}{\gamma\cosh\lambda'} \ , \qquad \text{(A18)}$$

$$\left[\frac{1}{Z_f}\frac{\partial^2 Z_f}{\partial a\partial\lambda}\right]_{n\to\infty}=fN(fN-1)\frac{e^{-\lambda'}}{2\gamma(\cosh\lambda')^2}e^{-\mu}, \tag{A19}$$

$$\left[\frac{1}{Z_f}\frac{\partial^2 Z_f}{\partial b\partial\lambda}\right]_{n\to\infty}=fN(fN-1)\frac{e^{-\lambda'}}{2\gamma(\cosh\lambda')^2}e^{\mu}, \tag{A20}$$

$$\left[\frac{1}{Z_f}\frac{\partial^2 Z_f}{\partial\lambda^2}\right]_{n\to\infty}=fN(fN-1)\frac{1}{(\gamma\cosh\lambda')^2}, \tag{A21}$$

(2) $\lambda'<\mu$:

$$\left[\frac{1}{n}\ln Z_f\right]_{n\to\infty}=fN\mu r, \tag{A22}$$

$$\left[\frac{1}{Z_f}\frac{\partial Z_f}{\partial a}\right]_{n\to\infty}=fNe^{-\mu}, \tag{A23}$$

$$\left[\frac{1}{Z_f}\frac{\partial Z_f}{\partial b}\right]_{n\to\infty}=\left[\frac{1}{Z_f}\frac{\partial^2 Z_f}{\partial a\partial\lambda}\right]_{n\to\infty}=\left[\frac{1}{Z_f}\frac{\partial^2 Z_f}{\partial b\partial\lambda}\right]_{n\to\infty}=0. \tag{A24}$$

$$\left[\frac{1}{Z_f}\frac{\partial Z_f}{\partial\lambda}\right]_{n\to\infty}=\left[\frac{1}{Z_f}\frac{\partial^2 Z_f}{\partial\lambda^2}\right]_{n\to\infty}=0. \tag{A25}$$

APPENDIX B: FLAVOR STRUCTURE OF THE $1/g^2$ AND $1/d$ CORRECTIONS

In this section we calculate the flavor tensor structure of the averages over two and four fermionic fields with respect to the generating functional:

$$R_f(\lambda_x,a_x,b_x)=\int\prod_{t\ \text{links}}[dU]\prod_{x,a}[d\bar\chi_a(x)d\chi_a(x)]\exp\left[-\sum_{x,y}\bar\chi_a(x)\left[\frac{\gamma}{2}a_x U_{xy}\delta_{x,y-\hat t}-\frac{\gamma}{2}b_x U^\dagger_{xy}\delta_{x,y+\hat t}\right]\chi_a(y)-\sum_x\lambda_x\bar\chi_a(x)\chi_a(x)\right], \tag{B1}$$

obtained from Z_{eff} after the replacement (2.5). Integration over $\bar\chi_a(x)$ and $\chi_a(x)$ in (B1) yields our partition function (2.6). $1/g^2$ corrections are proportional to the averages appearing in the expansion of the gauge sector combined with the fermion sector:

$$\delta F_1=C_1\sum_{\langle x,y\rangle}\langle\bar\chi_a(x)U_t(x)\chi_b(x+\hat t)\rangle\langle\bar\chi_b(y+\hat t)U_t^\dagger(y)\chi_a(y)\rangle, \tag{B2}$$

$$\delta F_2=C_2\sum_{\langle x,y\rangle}\sum_{\hat k}\langle\bar\chi_a(x)\chi_b(x)\rangle\langle\bar\chi_b(y)\chi_c(y)\rangle\langle\bar\chi_c(y+\hat k)\chi_d(y+\hat k)\rangle\langle\bar\chi_d(x+\hat k)\chi_a(x+\hat k)\rangle, \tag{B3}$$

$$\delta F_3=C_3\sum_{\langle x,y\rangle}\langle\bar\chi_a(x)\chi_b(x)\bar\chi_c(x)U_t(y)\chi_d(x+\hat t)\rangle\langle\bar\chi_b(y)\chi_a(y)\bar\chi_d(y+\hat t)U_t^\dagger(y)\chi_c(y)\rangle. \tag{B4}$$

In addition we have the $1/d$ correction due to the second term in Eq. (2.2):

$$\delta F_4=C_4\sum_{\langle x,y\rangle}\frac{N}{N+1}\langle\bar\chi_a(x)\chi_b(x)\bar\chi_c(x)\chi_d(x)\rangle\left[\frac{1}{N}\langle\bar\chi_b(y)\chi_a(y)\bar\chi_d(y)\chi_c(y)\rangle+\langle\bar\chi_b(y)\chi_c(y)\bar\chi_d(y)\chi_a(y)\rangle\right]. \tag{B5}$$

$\langle x,y\rangle$ denotes spatially neighboring sites at equal time and $\hat t$ and $\hat k$ are the unit vectors in temporal and spatial directions respectively. C_i are flavor-independent constants which can be found in Refs. [6,12]. Repeating flavor indices run from 1 to f. We need to relate the averages in (B2)–(B5) to the derivatives of R_f given by

$$\frac{1}{R_f}\frac{\partial R_f}{\partial a_x}=\langle\bar\chi_a(x)U_t(x)\chi_a(x+\hat t)\rangle, \tag{B6}$$

$$\frac{1}{R_f}\frac{\partial R_f}{\partial b_y}=\langle\bar\chi_a(y+\hat t)U_t^\dagger(y)\chi_a(y)\rangle, \tag{B7}$$

$$\frac{1}{R_f}\frac{\partial R_f}{\partial\lambda_x}=\langle\bar\chi_a(x)\chi_a(x)\rangle, \tag{B8}$$

$$\frac{1}{R_f}\frac{\partial^2 R_f}{\partial a_x\partial\lambda_x}=\langle\bar\chi_a(x)\chi_a(x)\bar\chi_b(x)U_t(y)\chi_b(x+\hat t)\rangle, \tag{B9}$$

$$\frac{1}{R_f}\frac{\partial^2 R_f}{\partial b_y\partial\lambda_y}=\langle\bar\chi_a(y)\chi_a(y)\bar\chi_b(y+\hat t)U_t^\dagger(y)\chi_b(y)\rangle, \tag{B10}$$

$$\frac{1}{R_f}\frac{\partial^2 R_f}{\partial\lambda_x^2}=\langle\bar\chi_a(x)\chi_a(x)\bar\chi_b(x)\chi_b(x)\rangle. \tag{B11}$$

It is easy to verify the following flavor tensor structure of our forms:

$$\langle \bar{\chi}_a(x)\chi_b(x)\rangle = \delta_{ab} g_1 \ , \tag{B12}$$

$$\langle \bar{\chi}_a(x)\chi_b(x)\bar{\chi}_c(x)\chi_d(x)\rangle = \left[\delta_{ab}\delta_{cd} - \frac{1}{N}\delta_{ad}\delta_{bc}\right] g_2 \ , \tag{B13}$$

$$\langle \bar{\chi}_a(x)U_t(x)\chi_b(x+\hat{t})\rangle = \delta_{ab} g_3 \ , \tag{B14}$$

$$\langle \bar{\chi}_a(x)\chi_b(x)\bar{\chi}_c(x)U_t(y)\chi_d(x+\hat{t})\rangle = \left[\delta_{ab}\delta_{cd} - \frac{1}{N}\delta_{ad}\delta_{bc}\right] g_4 \ , \tag{B15}$$

and similar expressions for the averages containing $U_t^\dagger$. The functions g_i are flavor scalars. Combining now Eqs. (B2)–(B11) with Eqs. (B12)–(B15) we find

$$\delta F_1 = \frac{1}{f} C_1 \sum_{\langle x,y\rangle} \frac{1}{R_f}\frac{\partial R_f}{\partial a_x}\frac{1}{R_f}\frac{\partial R_f}{\partial b_y} \ , \tag{B16}$$

$$\delta F_2 = \frac{1}{f^3} C_2 \sum_{\langle x,y\rangle} \sum_{\hat{k}} \frac{1}{R_f}\frac{\partial R_f}{\partial \lambda_x}\frac{1}{R_f}\frac{\partial R_f}{\partial \lambda_y} \times \frac{1}{R_f}\frac{\partial R_f}{\partial \lambda_{x+\hat{k}}}\frac{1}{R_f}\frac{\partial R_f}{\partial \lambda_{y+\hat{k}}} \ , \tag{B17}$$

$$\delta F_3 = \left[\frac{N-1}{fN-1}\right]^2 C_3 \sum_{\langle x,y\rangle} \frac{1}{R_f}\frac{\partial^2 R_f}{\partial a_x \partial \lambda_x}\frac{1}{R_f}\frac{\partial^2 R_f}{\partial b_y \partial \lambda_y} \ , \tag{B18}$$

$$\delta F_4 = \frac{(N-f)(N-1)}{f(fN-1)^2} C_4 \sum_{\langle x,y\rangle} \frac{1}{R_f}\frac{\partial^2 R_f}{\partial \lambda_x^2}\frac{1}{R_f}\frac{\partial^2 R_f}{\partial \lambda_y^2} \ . \tag{B19}$$

From these expressions we derive Eqs. (2.12)–(2.15).

[1] E. Dagotto, A. Moreo, and U. Wolff, Phys. Rev. Lett. **57**, 1292 (1986).
[2] A. Gocksch, Phys. Rev. Lett. **61**, 2054 (1988).
[3] F. Karsch and K.-H. Mütter, Nucl. Phys. **B313**, 541 (1989).
[4] I. Barbour, N.-E. Behilil, E. Dagotto, F. Karsch, A. Moreo, M. Stone, and H. W. Wyld, Nucl. Phys. **B275**, 296 (1986).
[5] N. Bilić and K. Demeterfi, Phys. Lett. B **212**, 83 (1988).
[6] N. Bilić, K. Demeterfi, and B. Petersson, Bielefeld Report No. BI-TP 91/18, 1991 (unpublished).
[7] G. Boyd, J. Fingberg, F. Karsch, L. Kärkkainen, and B. Petersson, Nucl. Phys. B (to be published).
[8] For a recent review, see B. Petersson, in *Quark Matter 90*, Proceedings of the Conference, Menton, France, 1990, edited by J. Blaizot *et al.* [Nucl. Phys. **A525**, 237c (1991)].
[9] R. Pisarski and F. Wilczek, Phys. Rev. D **29**, 338 (1984).
[10] H. Gausterer and S. Sanielevici, Phys. Lett. B **209**, 533 (1988).
[11] P. Damgaard, N. Kawamoto, and K. Shigemoto, Nucl. Phys. **B264**, 1 (1986).
[12] G. Fäldt and B. Petersson, Nucl. Phys. **B265** [FS15], 197 (1986).
[13] A. Gocksch, Phys. Rev. D **37**, 1014 (1988).
[14] P. E. Gibbs, Phys. Lett. B **182**, 369 (1986).
[15] J. C. Vink, Nucl. Phys. **B323**, 399 (1989).
[16] I. M. Barbour and Z. A. Sabeur, Nucl. Phys. **B342**, 269 (1990).
[17] A. Hasenfratz and D. Toussaint, Tucson Report No. AZPH-TH/91-21 (unpublished).
[18] E.-M. Ilgenfritz and J. Kripfganz, Z. Phys. C **29**, 79 (1985).
[19] P. H. Damgaard, D. Hochberg, and N. Kawamoto, Phys. Lett. **158B**, 239 (1985).
[20] A. Gocksch and M. Ogilvie, Phys. Rev. D **31**, 877 (1985).
[21] H. Kluberg-Stern, A. Morel, and B. Petersson, Nucl. Phys. **B215**, 527 (1983).
[22] F. Karsch and I. O. Stamatescu, Phys. Lett. B **227**, 153 (1989).
[23] J. Gasser and H. Leutwyler, Phys. Lett. B **184**, 77 (1987); **188**, 477 (1987).
[24] B. A. Campbell, J. Ellis, and K. A. Olive, Phys. Lett. B **235**, 325 (1990).
[25] J. B. Kogut, J. Polonyi, H. W. Wyld, and D. K. Sinclair, Phys. Rev. Lett. **54**, 1475 (1985).
[26] T. Jolicoeur, H. Kluberg-Stern, A. Morel, M. Lev, and B. Petersson, Nucl. Phys. **B235** [FS11], 455 (1984).
[27] F. Karsch and D. E. Miller, Phys. Rev. A **22**, 1210 (1980).